Anion-Initiated Trifluoromethylation by TMSCF₃: Deconvolution of the Siliconate−Carbanion Dichotomy by Stopped-Flow NMR/IR

Craig P. Johnston,[†,⊥] Thomas H. West,[†,⊥] Ruth E. Dooley,[†] Marc Reid,[†] Ariana B. Jones,[†] Edward J. King,[§] Andrew G. Leach,[‡] and Guy C. Lloyd-Jones*,[†]

†EaStChem, University of Edinburgh, Joseph Black Building, David Brewster Road, Edinburgh, EH9 3FJ, U.K.
‡School of Pharmacy and Biomolecular Sciences, Liverpool John Moores University, Byrom Street, Liverpool, L3 3AF, U.K.
§TgK Scientific Limited, 7 Long's Yard, St Margaret's Street, Bradford-on-Avon, BA15 1DH, U.K.

S Supporting Information

ABSTRACT: The mechanism of CF_3 transfer from R_3SiCF_3 (R = Me, Et, *i*Pr) to ketones and aldehydes, initiated by M^+X^- (<0.004 to 10 mol %), has been investigated by analysis of kinetics (variable-ratio stopped-flow NMR and IR), $^{13}C/^2H$ KIEs, LFER, addition of ligands (18-c-6, crypt-222), and density functional theory calculations. The kinetics, reaction orders, and selectivity vary substantially with reagent (R_3SiCF_3) and initiator (M^+X^-). Traces of exogenous inhibitors present in the R_3SiCF_3 reagents, which vary substantially in proportion and identity between batches and suppliers, also affect the kinetics. Some reactions are complete in milliseconds, others take hours, and others stall before completion. Despite these differences, a general mechanism has been elucidated in which the product alkoxide and CF_3^- anion act as chain carriers in an anionic chain reaction. Silyl enol ether generation competes with 1,2-addition and involves protonation of CF_3^- by the α-C−H of the ketone and the OH of the enol. The overarching mechanism for trifluoromethylation by R_3SiCF_3, in which pentacoordinate siliconate intermediates are unable to directly transfer CF_3^- as a nucleophile or base, rationalizes why the turnover rate (per M^+X^- initiator) depends on the initial concentration (but not identity) of X^-, the identity (but not concentration) of M^+, the identity of the R_3SiCF_3 reagent, and the carbonyl/R_3SiCF_3 ratio. It also rationalizes which R_3SiCF_3 reagent effects the most rapid trifluoromethylation, for a specific M^+X^- initiator.
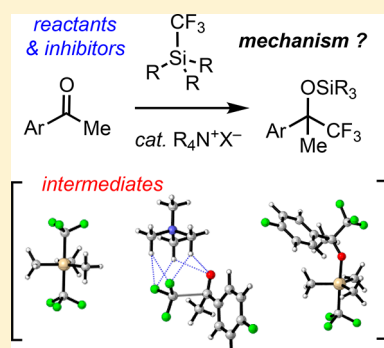
INTRODUCTION

The inclusion of fluorine substituents in organic molecules is of pivotal importance to developments in, *inter alia*, pharmaceuticals,[1] agrochemicals,[2] electronics,[3] materials chemistry,[4] polymers,[5] synthesis,[6] and catalysis.[7] The transfer of a formally nucleophilic CF_3-moiety to an electrophile is a preeminent method for the synthesis of trifluoromethylated compounds.[8] Conditions range from base-mediated reactions with fluoroform (CF_3H)[9] through to finely tuned borazine-based CF_3 carriers recently reported by Szymczak.[10] In 1989, Ruppert reported that TMSCF₃ (**1a**)[11] undergoes addition to aldehydes and ketones in the presence of 10 mol % KF.[12] A faster process, using a soluble initiator (Bu₄NF·*x*H₂O; 0.6 mol %, TBAF) was reported soon after, by Prakash and Olah.[13] Acidic workup affords the corresponding trifluoromethylated alcohols in good yield, Scheme 1.

Scheme 1. Trifluoromethylation of Ketones/Aldehydes[12,13a]

R = Ar, alkyl, vinyl, alkynyl, H
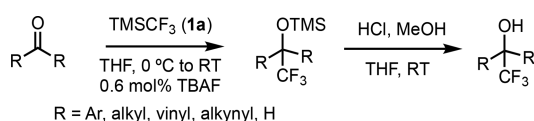
This mild and selective process[14] swiftly became adopted for the preparation of trifluoromethyl-carbinols,[15] including enantioselective additions involving enantiopure ammonium salts as initiators.[16] Indeed, over the past decade there has been an explosion of interest[17] in CF_3 transfer from TMSCF₃ (**1a**) to carbon (e.g., carbonyls,[14−17] imines,[18] vinyl halides,[19] and aromatics[20]) and to heteroatoms such as sulfur,[21] selenium,[22] phosphorus,[23] boron,[24] iodine,[25] and bismuth.[26] The formal loss of fluoride from CF_3 to facilitate electrophilic TMSCF₂ transfer[27] or carbenoid CF_2 transfer[28] has also been developed, as have numerous metal-mediated and -catalyzed processes involving CF_3 derived from TMSCF₃ (**1a**).[29]

Despite anion-initiated trifluoromethylation by **1a** having become a mainstream synthetic method,[17−26] surprisingly little detail has emerged on the mechanism of CF_3 transfer, under the conditions of application, Scheme 1.[30] Various mechanistic dichotomies, including, *inter alia*, fluoride initiation versus fluoride catalysis, and siliconate versus carbanion[23a] pathways, have been noted by Denmark[30a] and by Reich,[30b] both of whom emphasize the lack of salient kinetic data.

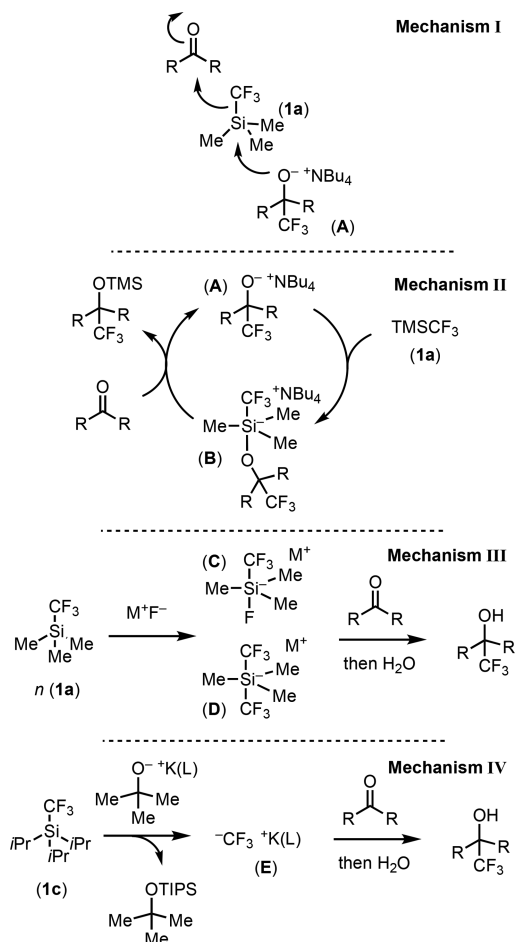Herein we report the first detailed study of the mechanism of anion-initiated CF$_3$ transfer from TMSCF$_3$ (**1a**) to ketone and aldehyde electrophiles.[12,17] The *in situ* NMR/IR investigations include analysis of reaction kinetics, selectivity, and side reactions and the contrasting behavior of homologues triethylsilyl (TES) (**1b**) and triisopropylsilyl (TIPS) (**1c**). Throughout the investigation, the kinetic studies have both informed and been directed by density functional theory (DFT) analysis of proposed intermediates. What emerges is a nuanced kinetic landscape in which trifluoromethyl transfer proceeds via a carbanion pathway (CF$_3^-$), with the rate dictated by the identity of the electrophile, the concentration of the initiating anion, the identity of the initiator counter-cation, the electrophile/R$_3$SiCF$_3$ (**1**) concentration ratio, and the identity of the reagent (**1a**−**c**).

■ RESULTS AND DISCUSSION

1. Prior Studies. In early studies, a termolecular anionic chain reaction (mechanism I, Scheme 2) was suggested for trifluoromethylation by **1a**.[13a] This was later expanded to a two-step process (mechanism II), where a pentacoordinate alkoxy-siliconate (**B**) delivers CF$_3$ to the ketone and in doing so liberates the *O*-silylated product.[14] Mechanism II has been extensively adopted in the design and interpretation of asymmetric trifluoromethylation.[16,29,31]

In 1999, Naumann[32] and Kolomeitsev and Röschenthaler[33] independently reported on the reaction of a range of soluble fluoride sources (e.g., [Me$_4$N]$^+$F$^-$) with TMSCF$_3$ (**1a**) at low temperature. Detailed ^{1}H, ^{13}C, ^{19}F, and ^{29}Si NMR analysis identified the products as pentacoordinate complexes [Me$_3$Si-(F)(CF$_3$)]$^-$M$^+$ (**C**) and [Me$_3$Si(CF$_3$)$_2$]$^-$M$^+$ (**D**). Both complexes decompose above −20 °C.[32,34] The speciation (**C**/**D**) is dependent on the stoichiometry (M$^+$F$^-$/**1a**), and the structure of **D** was confirmed by single-crystal X-ray diffraction. Addition of cyclohexanone at −60 °C, followed by hydrolysis, afforded the corresponding trifluoromethylated alcohol, mechanism III.[32,35]
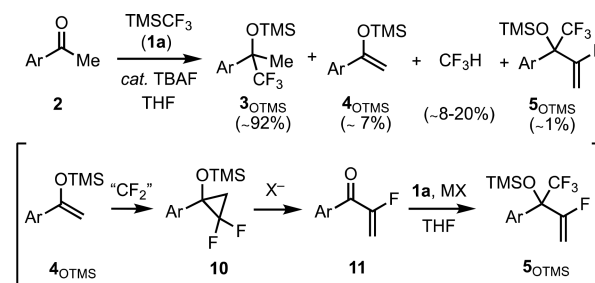
In 2014, Prakash[36] showed that the elusive[37] trifluoromethyl anion(oid)[38] can be detected *in situ* (^{13}C, ^{19}F NMR) at low temperatures after addition of KO*t*Bu/18-crown-6 to **1a**. With the much bulkier reagent TIPSCF$_3$ (**1c**), the generation of ion-paired [K(18-c-6)]$^+$[CF$_3$]$^-$ (**E**) proceeds quantitatively at −78 °C over a period of 30 min. Subsequent addition of PhCOMe (11 equiv) or PhCHO (4 equiv) afforded CF$_3$-addition products (22−68%) after quenching with H$_2$O, mechanism IV.[36] In 2015, Grushin[38] demonstrated that use of crypt-222 (**L**, Scheme 2) facilitates generation of the free CF$_3^-$ carbanion, a tetrahydrofuran (THF) solution-phase "non-covalently bound ionic species".[38] The structure of the highly air- and temperature-sensitive salt, [K(crypt-222)]$^+$[CF$_3$]$^-$ (**E**), was confirmed by single-crystal X-ray diffraction.[38,39]

The pioneering studies summarized above have been highly enlightening regarding the structure and stability of penta-coordinate (trifluoromethyl)siliconates (**C**, **D**)[32,33] and their ability to release the trifluoromethane anion(oid) (**E**) under specific conditions.[36,38] However, they do not yield direct detail on the kinetics and mode of transfer of CF$_3$ from TMSCF$_3$ (**1a**) to a carbonyl electrophile, using a catalytic fluoride-based initiator (M$^+$X$^-$), at ambient temperature.[12,13]

2. Preliminary Investigations. We began by studying the reaction of TMSCF$_3$ (**1a**) with aldehydes and ketones in THF, chlorobenzene, and dimethylformamide (DMF). After addition of catalytic quantities (0.1 to 1 mol %) of TBAF, ^{19}F NMR readily facilitated analysis of the proportions of residual reagent (**1a**) and the [1,2]-addition products. The reaction of 4-fluoroacetophenone (**2**) in THF at ambient temperatures proved ideal, the additional ^{19}F nucleus allowing simultaneous analysis of reagent (**1a**; 0.48 M), substrate (**2**; 0.40 M), and product (**3**$_{OTMS}$), Scheme 3.

Reactions were assembled manually in 5 mm NMR tubes in the glovebox prior to analysis *in situ* by ^{19}F NMR. Three side-

Scheme 2. Mechanisms I−IV for Anion-Induced Trifluoromethylation of Ketones Using Ruppert's Reagent (1a)[11] and Homologues[a]

^{a}L = 18-c-6, crypt-222. See text for full discussion.

Scheme 3. Trifluoromethylation of Ketone 2[a]

^{a}Ar = 4−F−C$_6$H$_4$.

products were identified: fluoroform (CF_3H), the silylenol ether (4_{OTMS}), and a homologated addition product (5_{OTMS}). Reactions conducted in d_8-THF proceeded analogously and generated CF_3H, not CF_3D.[40] The identity of 5_{OTMS}, which was confirmed by independent synthesis, is consistent with difluorocyclopropanation of silylenol ether 4_{OTMS} to generate **10**, followed by a known[41] anion-induced ring-opening elimination to give fluoroenone **11** and subsequent 1,2-selective[12] trifluoromethylation. Addition of independently synthesized[42] **10** to the reaction (Scheme 3) generated 5_{OTMS}.

Reaction rates and extent of fluoroform generation (Scheme 3) were found to vary significantly between batches of TBAF (1 M, THF, ~5 wt % H_2O). Replacing TBAF with anhydrous $[Bu_4N][Ph_3SiF_2]$ (TBAT)[43] gave more reproducible data. However, the fast turnover precluded detailed kinetic analysis; this aspect was addressed using stopped-flow methods, *vide infra*. Nonetheless, ^{19}F NMR analysis revealed that CF_3H is liberated in two distinct phases. The first is an initial burst of extremely rapid CF_3H generation and arises from TBAT-catalyzed reaction of $TMSCF_3$ (**1a**) with traces of adventitious water.[44] The second phase of CF_3H generation proceeds in concert with reaction of the ketone (**2**) and directly correlates with the rate of generation of silylenol ether (4_{OTMS}), as confirmed by [2]H-labeling (d_3-**2** → CF_3D + d_2-4_{OTMS}). The selectivity (3_{OTMS} versus 4_{OTMS}) is discussed later.

3. Stability, Inhibition, and Tests for Radicals. The stability of the reaction system after complete consumption of the limiting reagent (ketone **2** or $TMSCF_3$ **1a**) was found to depend on which one was in excess. Reactions in which **2** was in excess underwent turnover on addition of further $TMSCF_3$ **1a**, even after a period of many hours. In contrast, for reactions where **1a** was in excess, additional **2** had to be added within a few minutes to fully reinstate turnover (see SI), consistent with the known instability of pentacoordinate (trifluoromethyl)-siliconates, e.g., **C** and **D**, at ambient temperatures.[32−34] Further tests established that the reactions were not sensitive to exogenous water *per se*, as they rapidly self-dehydrated via generation of CF_3H + hexamethyldisiloxane, prior to reaction of the ketone (**2**).[45] The rates were unaffected by visible light, by exogenous product (3_{OTMS}), and by CF_3H. Deliberate sparging of the normal reaction mixture (**1a/2**/TBAT 0.15 mM, 0.038 mol %, THF, Scheme 3) with air caused complete inhibition of turnover, but only when a sufficient volume of CO_2 (~400 ppm) had been added to convert the active anion(s) into trifluoroacetate (i.e., $[Bu_4N][CF_3CO_2]$, detected by ^{19}F NMR). Separate controls confirmed that the rate of trifluoromethylation is unaffected by CO_2-scrubbed air and that $[Bu_4N][CF_3CO_2]$ is not effective as an initiator.

However, the reactions were inhibited by addition of the persistent radical tetramethylpiperidinooxy (TEMPO). Indeed, just 0.45 mM TEMPO induced complete inhibition of the reaction of **1a** with **2**, initiated by 0.15 mM TBAT (Scheme 4, A). In contrast, TEMPO had a negligible impact on reactions employing TES (**1b**) and TIPS (**1c**), even when present at much higher concentrations (80 mM TEMPO); the origins of this profound difference in behavior is discussed later. Nonetheless, further tests for discrete radical intermediates[46,47] were conclusively negative: 4-F-benzophenone (**12**) exclusively underwent 1,2-addition (Scheme 4, B),[48,49] cyclopropyl ketones (**6/7**) reacted without any trace of competing ring-opening[50] (Scheme 4, C), and competition between ketone **2** and 4-biphenyl methyl ketone for limiting $TMSCF_3$ (**1a**) favored **2** (k_{rel} = 1.93).[51]

Scheme 4. Tests for Radical Intermediates
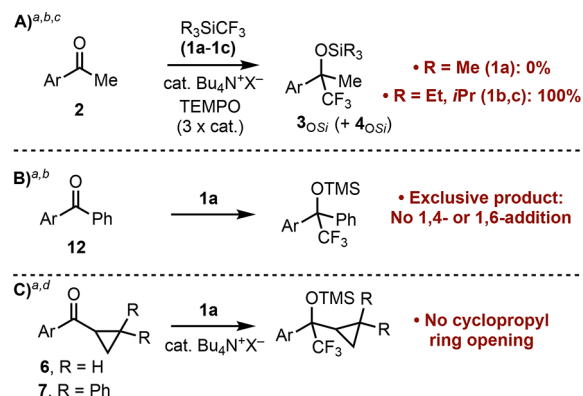
^{a}Ar = 4-F-C_6H_4; ketone (**2**, **6**, **12**, 0.40 M; **7**, 0.2 M), **1a**−**c** (1.2 equiv.), THF, 21 °C. ^{b}catalyst = TBAT (for **A**) or TBAF (for **B**). ^{c}TEMPO (0.12 mol %, 0.45 mM; up to 80 mM with **1b,c**). ^{d}TBAF (1 mol %).
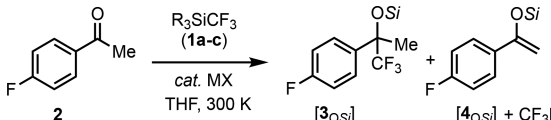
4. General Effects of Initiator on Rate and Selectivity. A range of initiators (M^+X^-) were tested and found to strongly impact the reaction outcome. In the majority of cases, the reactions initiated "instantly" and the identity of X^- had no influence on the rate[52] or selectivity ($3_{OTMS}/4_{OTMS}$). Specific effects were found to be dictated by the identity of the countercation (M^+), Table 1.

Reactions where $M^+ = K^+$ and Cs^+ proceeded rapidly to completion, with higher selectivity for $3_{OTMS}/4_{OTMS}$ compared to Bu_4N^+. Reactions stalled when the cation was Li^+ or Na^+.[53] For the K^+-mediated system, the rate was strongly attenuated by addition of 18-crown-6 or crypt-222, with the latter causing turnover to become slower and less selective ($3_{OTMS}/4_{OTMS}$) than reactions initiated by TBAT (countercation Bu_4N^+). The identity of M^+ was also found to affect the degree of charge development (ρ ranging from 1.8 to 3.0) in the ketone (R = Me, Scheme 5) at the product-determining transition state for CF_3 transfer. Benzaldehydes (R = H) behaved analogously.

5. Effect of Silyl Reagent on Rate and Selectivity. To further probe the CF_3 transfer process, we compared $TMSCF_3$ (**1a**) with $TESCF_3$ (**1b**) and $TIPSCF_3$ (**1c**), Table 1. The effects of changing the reagent were counterintuitive and initially misleading regarding the mechanism of CF_3 transfer, *vide infra*. Reactions employing $TESCF_3$ (**1b**) gave lower selectivity ($3_{OTES}/4_{OTES} \approx 1.5/1$) and proceeded very rapidly, even at low TBAT concentrations (150 μM, 0.0375 mol %; below this, reactions failed to initiate). In contrast, reactions employing $TIPSCF_3$ (**1c**) proceeded very slowly, requiring high initiator concentrations to proceed efficiently (>1.5 mM, 0.375 mol %) and gave even lower selectivity ($3_{OTIPS}/4_{OTIPS} \approx 1/1$).

Further insight was afforded by reaction of a 50/50 mixture of $TMSCF_3$ (**1a**) and $TESCF_3$ (**1b**), initiated by TBAT (75 μM, 0.019 mol %), Figure 1. The first 4 min of reaction is dominated by turnover of $TMSCF_3$ (**1a**) to generate $3_{OTMS}/4_{OTMS}$, and upon near-complete consumption of **1a**, turnover accelerates substantially as the $TESCF_3$ (**1b**) is engaged to generate $3_{OTES}/4_{OTES}$. The data indicate that the less-hindered reagent (**1a**) monopolizes the anion, but undergoes slower turnover.

Under conditions where anion-induced reactions of TMS (**1a**), TES (**1b**) and TIPS (**1c**) with **2** could be conducted slowly enough to be accurately monitored *in situ* by ^{19}F NMR,

Table 1. Examples of Effect of Initiator M⁺ and Reagent (1a−c) on Selectivity (3₀ₛᵢ/4₀ₛᵢ) and Rate of Trifluoromethylation of 2

| M⁺	[M⁺X⁻]₀, mM	TMS 1a 3/4[a] (time)[b]	TES 1b 3/4[a] (time)[b]	TIPS 1c 3/4[a] (time)[b]
[Bu₄N]⁺	1.5	12/1 (<90 s)	1.5/1 (<90 s)	1/1 (30 min)
[K]⁺	0.15	36/1 (<90 s)	3.0/1[c] (30 min)	NR
[K(L)]⁺[d]	1.5	6.6/1 (6 min)	2.4/1 (<90 s)	1/1 (3.6 min)

[a]Selectivity $3_{OSi}/(4_{OSi}+CF_3H)$ measured *in situ* by ¹⁹F NMR after manual assembly in an NMR tube; selectivity is independent of X⁻. [b]times indicated are for >97% conversion of **2**, at 300 K. [c]85% conversion. [d][K(L)]⁺ = K(crypt-222)]⁺, generated *in situ* from KOPh + crypt-222. NR = No reaction.
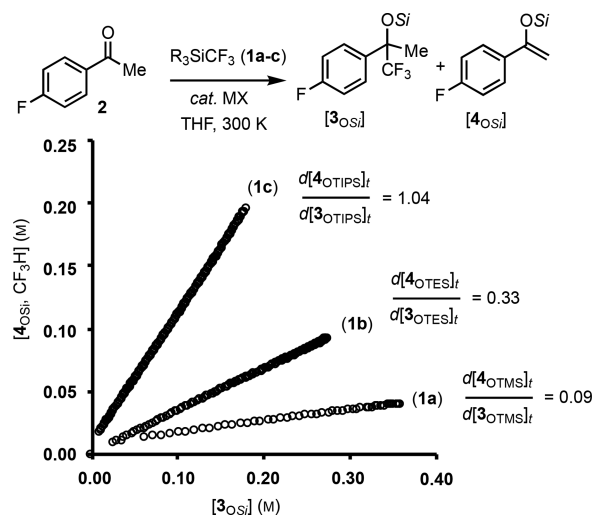
Scheme 5. Effect of Initiator M⁺ on Reaction Constant (ρ)

M⁺	ρ(Me)	ρ(H)
Na	1.76	--
K	1.79	1.27
Cs	2.00	--
K(18-c-6)	2.00	2.01
NBu₄	2.62	2.35
K(crypt-222)	2.98	2.55

$\rho = \sigma \log_{10}(k_Z/k_F)$ [¹⁹F NMR]
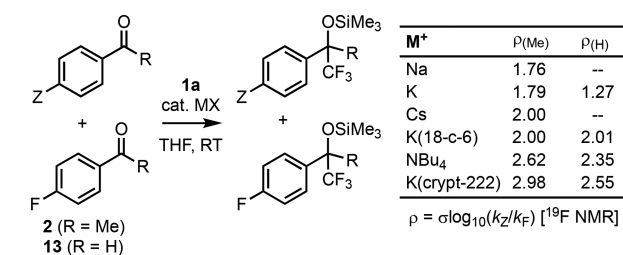
[a](i) 4-Z-C₆H₄COR (0.2 M), **2/13** (0.2 M), **1a** (0.04 M), PhF (0.4 M), MX (0.00015 M; 0.038 mol %). Z = Ph, OMe, CF₃, Me, Br. Hammett rho values calculated from product ratios; see SI.
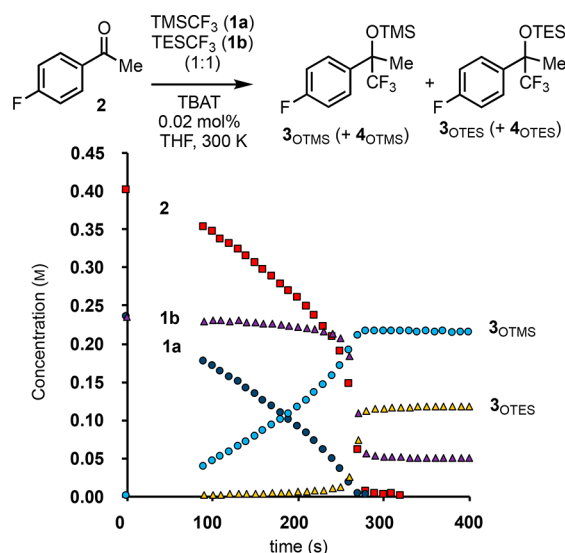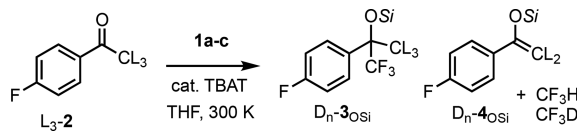

Figure 1. Competition between TMSCF₃ (**1a**)/TESCF₃ (**1b**); see text for full discussion. Reaction conditions: **2** (0.4 M), **1a** (0.24 M), **1b** (0.24 M), PhF (internal standard, 0.4 M), TBAT (75 μM, 0.019 mol %); ¹⁹F NMR analysis, manual assembly.

Figure 2. Constant ratio of $[4_{OSi}]_t/[3_{OSi}]_t$. Conditions: **2** (0.4 M), **1a−c** (0.48 M), PhF (internal standard, 0.4 M), MX (TBAT 150 μM for **1a**; KOPh 0.15 mM for **1b**, TBAT 1.5 mM for **1c**).

Reactions with labeled ketone (aryl-d_4-**2**; CD₃-**2**; ¹³CO-**2**) were also instructive, Table 2. Reaction of TMSCF₃ (**1a**) with

Table 2. KIEs and ²H Exchange in the Reaction of Ketone 2[a,b]

CL₃ (reagent)	1a−c	2,3₀ₛᵢ	k_H/k_D	
CH₃ (¹³C=O)	1a	CH₃		$(k_{12C}/k_{13C} = 1.008)^c$
CH₃ (C₆D₄)	1a	CH₃	1.038[d]	
CD₃	1a	CD₃	6.4	(3/4₀ₜₘₛ = 72/1)
CD₃ + CH₃	1a	CD₃/CH₃ only	6.1	(rate: CF₃H/CF₃D)
CD₃	1b	CD₃	3.1	(3/4₀ₜₑₛ = 4.3/1)
CD₃ + CH₃	1b	partial CD₃₋ₙ/Hₙ		(3/4₀ₜₑₛ = 2.3/1)
CD₃	1c	CD₃	1.1	(3/4₀ₜᵢₚₛ = 1.1/1)
CD₃ + CH₃	1c	full CD₃₋ₙ/Hₙ	1.0	(rate: CF₃H/CF₃D)

[a]Ketone (**2**/²H₃-**2**; 0.40 M), **1a−c** (0.48 M), THF, 300 K. TBAT (0.04 mol %, 0.15 mM). [b]Selectivity $3_{OSi}/(4_{OSi} + CF_3H/D)$ and exchange measured *in situ* by ¹⁹F NMR analysis. [c]KIE determined by competition with *aryl*-d_4-**2**. [d]²H KIE induced by aryl-deuteration, determined by competition with unlabeled **2**.

the ratios of enol/addition product ($4_{OSi}/3_{OSi}$) were all *constant* throughout the reaction evolution, Figure 2. A further distinction originated from the impact of the addition of crypt-222 to KOPh-initiated reactions. As noted above, for TMSCF₃ (**1a**) the incarceration of the K⁺ in the crypt-222 ligand substantially attenuates the rate and selectivity. In stark contrast, for TIPSCF₃ (**1c**), turnover is substantially *accelerated* by addition of crypt-222 to inhibit K⁺/anion pairing.

2 initiated by TBAT (0.15 mM) proceeds with a very low ^{13}C kinetic isotope effect (KIE), determined by competition with aryl-d_4-2, after normalizing for the effect of aryl deuteration.

In contrast, a substantial primary ^2H KIE, determined from $[CF_3D]$ versus $[d_3$-$3_{OSi}]$, as in Figure 2, increases the addition/ enol selectivity ($k_H/k_D = 6.4$). Reactions of mixtures of 2 and d_3-2 proceeded with no detectable scrambling of D/H between $2/D_3$-2 during turnover, provided that $[1a]_0 > [2]_0$, and again proceeded with a high KIE ($k_H/k_D = 6.1$). With TESCF$_3$ (1b) a moderate KIE ($k_H/k_D = 3.1$) was observed, with a trace of D/ H exchange between 2 and D$_3$-2 on co-reaction, and thus into products d_n-3/d_n-4. With TIPSCF$_3$ (1c) there was no significant KIE and a statistical mixture of isotopologues of d_n-2/3 ($n = 0-3$) was evident immediately after initiation of the reaction.[54]

6. Variable-Ratio Stopped-Flow NMR and IR. Detailed exploration of the kinetics of the trifluoromethylation by 1a required techniques for rapid acquisition of kinetic data (some systems had formal turnover frequencies well in excess of 5000 s^{-1}, *vide infra*) in a time- and material-efficient manner. Stopped-flow techniques are ideal for rapid and reproducible initiation and analysis of these reactions. However, the classic fixed-ratio dual input mode of operation ($A + B$; Figure 3a)
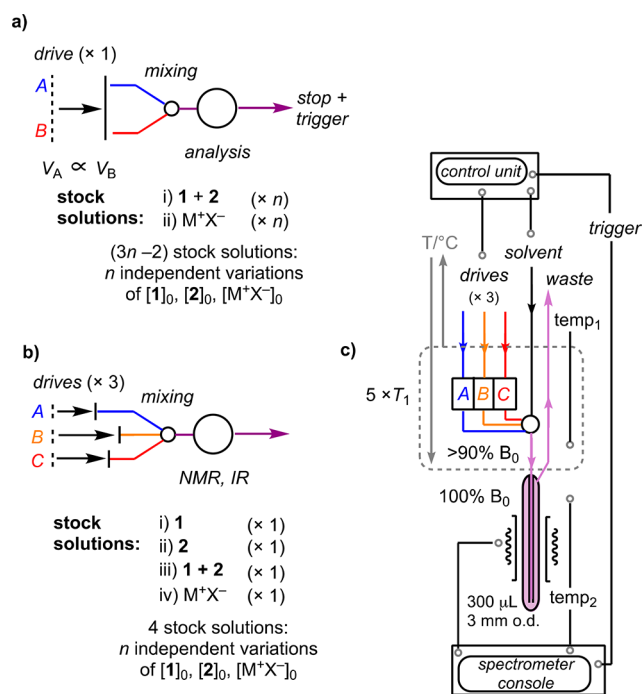
Figure 3. Schematic representations of (a) classic fixed-ratio dual input stopped-flow; (b) a variable-ratio triple-input design; and (c) variable-ratio stopped-flow NMR with thermostatic premagnetization of reactants (A, B, C), for >5 × T_1 at >90% (B_0).

requires separate solutions to be prepared for every variation in conditions. For a three-component process such as R$_3$SiCF$_3$ (1) + ketone 2 + initiator (M$^+$X$^-$), a very large number of stock solutions are required to study reactions with different concentrations of reactants and initiator.

To address this issue, we constructed a stopped-flow system, in which the delivered volumes of *three* solutions (A, B, C) are independently variable,[55] using a computer-controlled triple stepper-motor system, Figure 3b. This setup allowed systematic analysis of the kinetics across a wide range of initial

conditions, *using just four stock solutions*, mixing {i + iii + iv} varies $[2]_0$; mixing {ii + iii + iv} varies $[1]_0$; and mixing {iii + iv + THF} varies $[M^+X^-]_0$, while keeping the other species constant; see SI for full details. The new system was implemented in two modes: IR and NMR.[56] The former simply required adaptation of our recently developed thermostated ATR-FTIR stopped-flow cell,[57] replacing the dual mixing stage with a triple mixer and a gated reaction volume. The analogous setup for variable-ratio stopped-flow NMR required bespoke construction. The principles for continuous-flow NMR recently reported by Foley et al.[58] were employed for the basic design, such that the reaction vessel and associated components can be installed simply by insertion of the device into the sample transit of a standard unmodified NMR spectrometer. Nuclei premagnetization is facilitated in three independent reservoirs (A, B, C) located as close as possible to the magnetic field center, Figure 3c. The reservoirs connect at a tripodal-geometry mixer that discharges via a 0.5 mm i.d. glass capillary into a 3 mm external diameter 300 μL glass NMR flow-cell. The tube terminates at the base of the cell, with the waste outlet at the top. A fourth input to the mixer allows the system to be flushed with solvent between runs. Thermostating is achieved by passage of a heat-transfer medium (aqueous ethylene glycol), using an externally controlled recirculator, through an umbilical containing all stages of the stopped-flow circuit, except for the glass flow-cell, which is located within the spectrometer-thermostated probe head; precalibration ensures temp$_1$ = temp$_2$. During a typical stopped-flow (SF) "shot", a total of 600 μL is delivered through the flow-cell at a rate of 1–2 mL s^{-1}, fully displacing the previous contents and replacing it with 300 μL of freshly assembled reaction mixture; charging requires 70–130 ms (measured independently by UV–vis), with high-quality NMR spectra (N$_2$-cryoprobe) achievable immediately thereafter. Control of the timing of the NMR pulse sequence is achieved by a trigger signal, sent to the spectrometer console from the computer-controlled triple stepper-motor system, immediately after the 300 μL flow-cell has been freshly charged.

7. Kinetics of Trifluoromethylation by TMSCF$_3$ (1a) and TIPSCF$_3$ (1c). The kinetics of reactions initiated by M$^+$X$^-$, where M$^+$ = Bu$_4$N$^+$, K$^+$, and Cs$^+$, were studied in detail by SF-IR and SF-NMR across a wide range of concentrations of 1a, 2, and $[M^+X^-]_0$. For FTIR, the decay in the IR C–F stretching mode (1056 cm^{-1}) of the TMSCF$_3$ (1a) and the growth in C–F stretching mode (1165 cm^{-1}) of 3_{OTMS} were collected at scan rates of 14 or 28 s^{-1} with a resolution of 2 or 8 cm^{-1}, respectively. ^{19}F NMR analysis allowed detailed analysis of the reaction components, but was naturally more limited in terms of temporal resolution. For faster reactions, a technique involving the interleaving of a series of spectra from a sequence of stopped-flow NMR "shots" was employed, affording a higher virtual temporal resolution.

A key component in analysis of the kinetics was the dependence of the temporal-concentration evolution of the product (3_{OTMS}) on the concentration *ratio* of ketone 2 and TMSCF$_3$ (1a). Systematic studies of initial rates using TBAT led to an empirical rate equation for turnover frequency (TOF) in which the initiator (Bu$_4$N$^+$X$^-$) and ketone 2 are first order and the TMSCF$_3$ (1a) reagent approximately *inverse* first order (eq 1).[59] Control experiments in which the reactions were run in the presence of exogenous product (3_{OTMS}) confirmed that it does not act as an inhibitor.
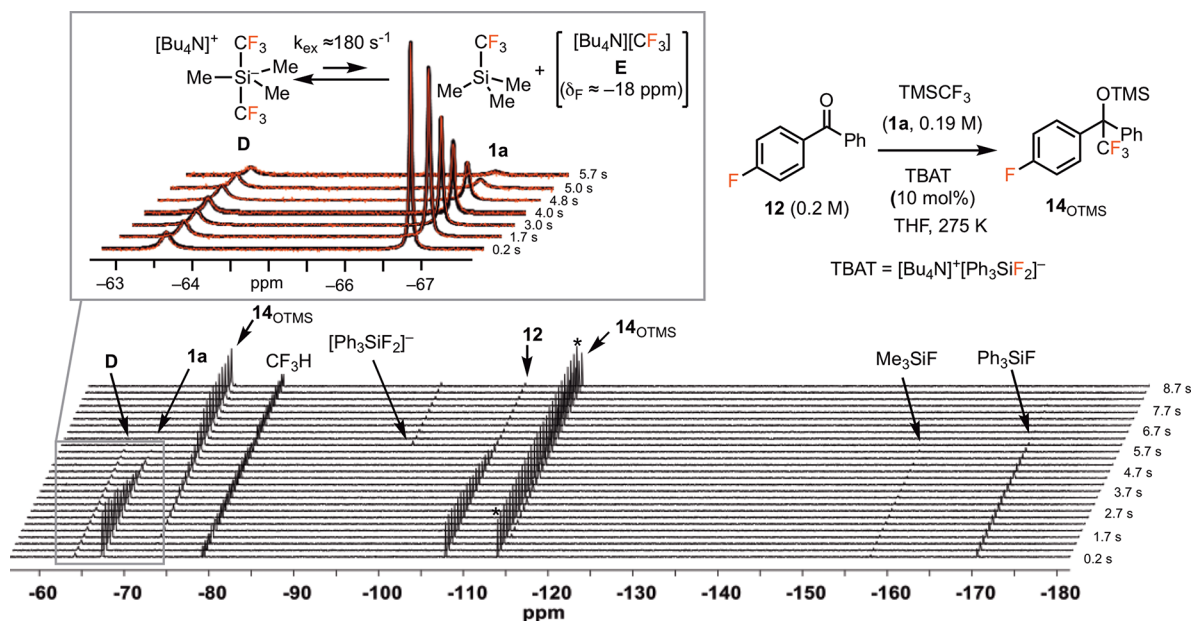
Figure 4. Selected spectra from stopped-flow ^{19}F NMR analysis of the reaction of 4-F-benzophenone **12** (0.20 M) with **1a** (0.19 M) in THF at 275 K after initiation by 10 mol % TBAT. Inset: Overlay of selected simulations[62] (black) of dynamic line-shape for **D/1a** with experimental spectra (red); **E** (δ_F −18 ppm) is undetected. (*) C_6H_5F is internal standard.

The inhibitory effect of the TMSCF$_3$ reagent **1a** (K_{i1}; eq 1) results in very distinctive temporal concentration profiles for the reaction, simulations of which are presented later. For example, when the initial ratio of reactants is equal ($[\mathbf{2}]_0 = [\mathbf{1a}]_0$), their ratio remains constant ($[\mathbf{2}]_t/[\mathbf{1a}]_t = 1$) throughout the reaction. What arises is an apparent pseudo-zero-order consumption of the reactants (TOF = k_{obs}) for the majority of the reaction evolution. Conversely, when there is an excess of ketone **2** over **1a**, the rate of turnover rises as a function of conversion, becoming very rapid in the final phases of reaction where $[\mathbf{2}]_t/[\mathbf{1a}]_t \gg 1$.

$$\text{TOF} \approx \frac{k_{rxn}[\text{M}^+\text{X}^-]_0[\mathbf{2}]_t(1-x_{EI})}{1 + K_{i1}[\mathbf{1}]_t} \approx k_{obs}\frac{[\mathbf{2}]}{[\mathbf{1}]} \quad (1)$$

$$\text{TOF} \approx \frac{k_{rxn}[\text{M}^+\text{X}^-]_0[\mathbf{1}]_t(1-x_{EI})}{1 + K_{i2}[\mathbf{2}]_t} \approx k_{obs}\frac{[\mathbf{1}]}{[\mathbf{2}]} \quad (2)$$

Systematic studies using M$^+$X$^-$ (M$^+$ = Li$^+$, Na$^+$, K$^+$, Cs$^+$), which induce very rapid turnover, proved more challenging. Reactions where M$^+$ = Li$^+$ and Na$^+$ stalled before completion and were not reproducible. KOPh and CsOPh initiated at very low concentrations, without an evident induction period, proceeded to completion, and provided reproducible kinetics. Study of the *initial* rates suggested higher-order dependencies on TMSCF$_3$ ($[\mathbf{1a}]_0$, again inverse) and on $[\text{M}^+\text{X}^-]_0$, with the ketone **2** remaining first-order. However, the reactions *evolve* with near-identical behavior to those initiated by TBAT (eq 1).[59] The dichotomy is indicative of the presence of exogenous inhibitor(s) in low concentration in the TMSCF$_3$ (**1a**) reagent that are not consumed during reaction. Increasing the initial concentration of the reagent ($[\mathbf{1a}]_0$) or decreasing the initiator concentration ($[\text{M}^+\text{X}^-]_0$) causes a greater mole fraction of exogenous inhibition (x_{EI}), eq 1.[59,60] Addition of $[\text{K}]^+[(\text{C}_6\text{F}_5)_4\text{B}]^-$, to provide an additional soluble K$^+$ source with a non-nucleophilic counteranion, had no impact on the kinetics of reactions initiated by KOPh, indicative that the rate is dependent on the initiating anion *concentration* and the

countercation *identity* (but not its concentration).[61] Addition of potassium-binding ligands attenuated the rates substantially, and with crypt-222, the system underwent turnover slower than with Bu$_4$N$^+$ (a 3 orders of magnitude rate reduction compared to free K$^+$).

The kinetics of trifluoromethylation of 4-fluorobenzaldehyde (**13**) by **1a** were also explored using TBAT as initiator. The aldehyde undergoes significantly faster trifluoromethylation than ketone **2** ($k_{ald}/k_{ket} \approx 80$, at 21 °C), requiring lower initial TBAT concentrations and causing the traces of exogenous inhibitor(s) in **1a** to complicate the kinetics.[59] Competing ketone **2** with aldehyde **13** (9/1 ratio) using stopped-flow ^{19}F NMR to analyze the transient substrate ratio (**2/13**) during the first 5−30 s of reaction indicated that the relative rate of trifluoromethylation is independent of $[\text{TBAT}]_0$ (96−384 μM) and **1a** (0.08 to 0.48 M). Overall, the data are indicative that aldehyde **13** follows the same general kinetics as ketone **2**, i.e., eq 1.[59,60] The rate of trifluoromethylation of ketone **2** using TIPSCF$_3$ (**1c**) was much slower than with **1a**. Again, the kinetics were impacted by exogenous inhibitor(s) in the reagent ($[\mathbf{1c}]_0$), the effect of which (x_{EI}) varied from batch to batch of **1c**; see SI. Using TBAT as initiator, the reactions evolve with a first-order dependency on the initiator and on the reagent ($[\mathbf{1c}]_t$), with inhibition by the ketone (K_{i2}; eq 2). In other words, the kinetic dependencies are the opposite to that found for **1a** (compare eqs 1 and 2), with reactions accelerating when there is an excess of **1c** over **2**. Reactions of **2** with **1c** initiated by KOPh were slower than those initiated by TBAT and were accelerated on addition of crypt-222; the opposite phenomena to those observed with **1a**.

8. Stopped-Flow ^{19}F NMR Analysis of Siliconate and Alkoxide Intermediates, Exchange Dynamics with TMSCF$_3$, and Initiator Regeneration. By use of 4-F-benzophenone (**12**; δ_F −107.0 ppm), which reacts slower than **2**, and reducing the reaction temperature to 275 K, the temporal speciation of the initiator-derived species (10 mol % TBAT) was monitored using stopped-flow ^{19}F NMR, Figure 4.
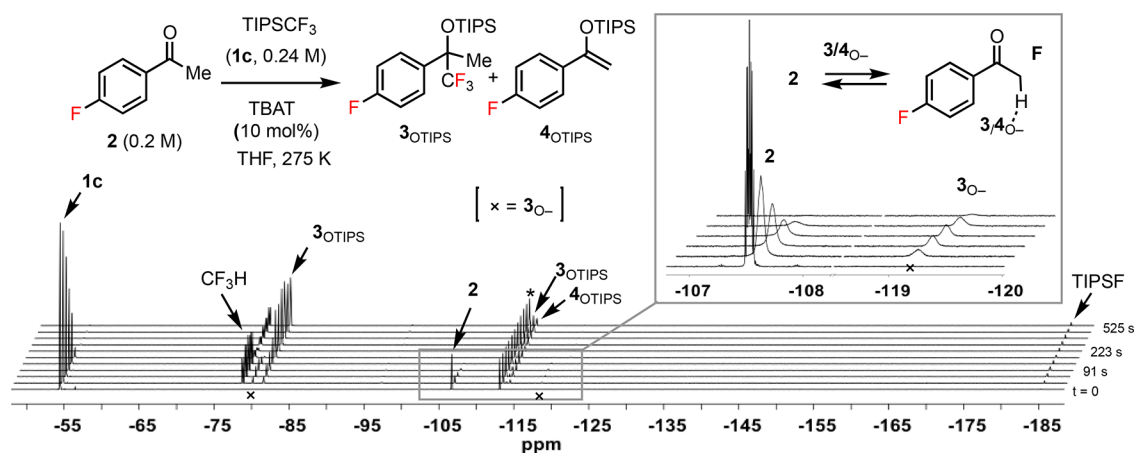
Figure 5. Selected spectra from *in situ* ^{19}F NMR analysis (manual assembly) of the reaction of 4-F-acetophenone **2** (0.20 M) with **1c** (0.24 M) in THF at 275 K after initiation by 10 mol % TBAT (t = 0, no TBAT). Inset: Line-broadening in ketone **2** and alkoxide 3_{O-}. (*) C_6H_5F is internal standard. (x) = 3_{O-}. Free 4_{O-} not located, possibly due to degenerate exchange with **2**. Ph_3SiF is not observed.
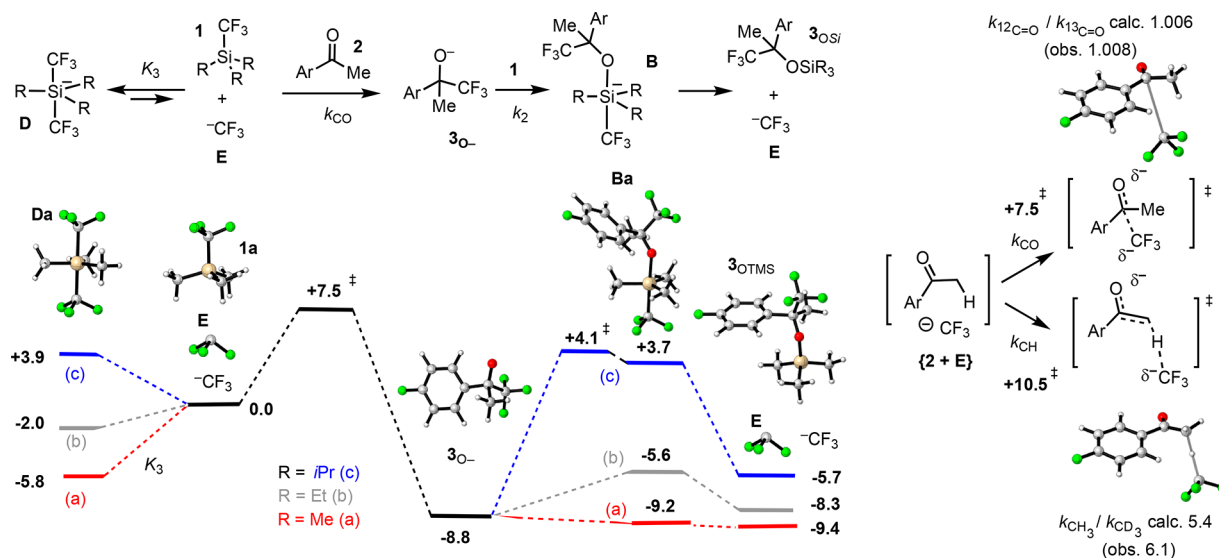

Figure 6. Selected structures and energies (M06L/6-31+G*; PCM (THF); standard state, 1 M; 298 K) of naked anions in the reaction of ketone **2** with R_3SiCF_3 **1a–c**. Energies have been normalized to $[CF_3^- + 1 + 2] = 0.00$ kcal mol^{-1}. See text, Figure 9, and the SI for discussion of the binding modes and effects of cations. The structures and energies of other potential intermediates examined, including hexacoordinate dianions and fluoride adducts, are provided in the SI.

The known but unstable hypervalent bis-CF$_3$-siliconate (**D**; δ_F −63.3 ppm)[32−34] is generated instantly. Integration against fluorobenzene (internal standard, δ_F −113.2 ppm) shows **D** to be present at 10 mol % and thus the predominant anion speciation. A key feature in the time series is the dynamic line-broadening in **D** that is constant throughout the reaction, but develops in the TMSCF$_3$ (**1a**) reagent (δ_F −66.6 ppm) as its concentration is depleted by the overall reaction with super-stoichiometric ketone **12**. In parallel with this is a marked acceleration in product generation (**14**$_{OTMS}$, δ_F −72.4 and −113.7 ppm), consistent with eq 1. After 6 s, the TMSCF$_3$ (**1a**) is fully consumed and TBAT (δ_F −97.4 ppm) is regenerated from Ph$_3$SiF/Me$_3$SiF. The dynamic line-broadening in **D/1a** can be satisfactorily simulated using a three-spin exchange process in which **D** is in rapid dissociative equilibrium ($k_{exch} \approx 180$ s^{-1}; $\Delta G^{\ddagger} \approx 13$ kcal mol^{-1}) with **1a** and a low concentration of (unobserved) [Bu$_4$N][CF$_3$] (**E**).[62] At 300 K, the line-broadening is very extensive and **D** short-lived.

Analogous experiments using TIPSCF$_3$ (**1c**) gave a very different outcome. Reactions conducted with **1c** at 275 K were slow enough to be followed using ketone **2** (δ_F −106.7 ppm), Figure 5. The ^{19}F NMR signal for **1c** remains sharp until **2** has been fully consumed. In contrast to reactions with **1a** (Figure 4) the alkoxide (3_{O-}; δ_F −118.4) is present in significant concentration and exhibits dynamic line-broadening (see inset in Figure 5). The signal for ketone **2** also exhibits dynamic line-broadening, immediately after addition of TBAT. On complete consumption of **2** (~120 s), the signals for remaining **1c** and CF$_3$H are broadened, presumably due to indirect exchange involving CF$_3^-$. After a further 300 s, **1c** is fully consumed and the CF$_3$H doublet becomes sharp again.

9. General Mechanism for Anion-Initiated CF$_3$ Transfer from R$_3$SiCF$_3$ to Ketones and Aldehydes. The data outlined in Sections 2 to 8 above (see SI for full details) indicate that the M$^+$X$^-$-initiated trifluoromethylation of ketone **2** by TMSCF$_3$ (**1a**) involves an electrophile−nucleophile reaction, in which the CF$_3$ transfer is accompanied by M$^+$.
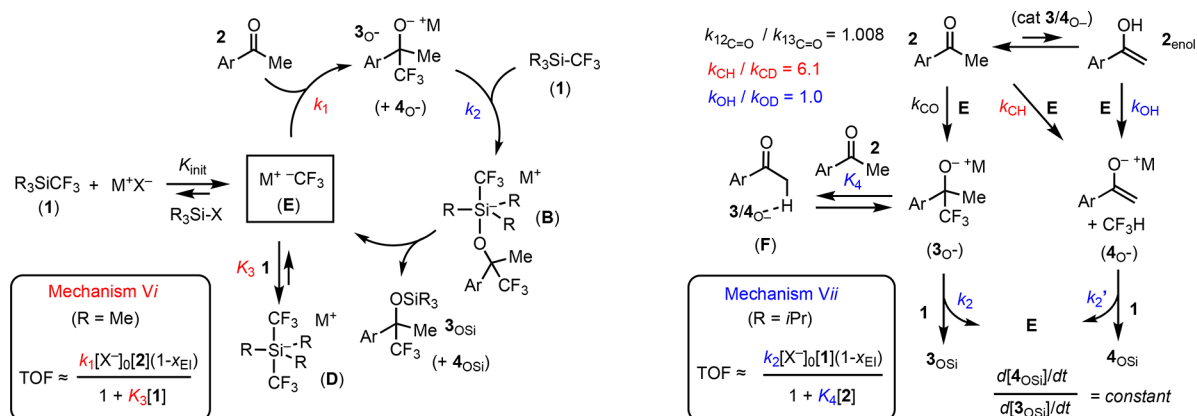
Figure 7. Mechanisms Vi and Vii: two extremes of general model V for the trifluoromethylation of ketones by R_3SiCF_3 reagents **1a–c**, in the presence of a catalytic quantity of initiator M^+X^-, with acetophenone as a generic reactant. Turnover frequency (TOF) equations are simplifications of a global approximation, where $k_1 = k_{CO} + k_{CH} + k_{OH}[2_{enol}]/[2]$, and the mole fraction of active anion quenched by unidentified exogenous inhibitor(s) in **1** is x_{EI}. Initiation (K_{init}) is not included in the rate equation. When M^+X^- is TBAT, initiation is reversible using **1a**. For nonenolizable ketones and aldehydes, k_{CH}, k_{OH}, and $K_4 = 0$.

Enolsilane 4_{OTMS} is also generated ($\leq 2\%$ when $M^+ = K^+$ and 7% when $M^+ = Bu_4N^+$) with coproduct CF_3H ($k_H/k_D = 6.1$). Using TIPSCF$_3$ (**1c**), approximately 50% of the product is 4_{OTIPS} and $k_H/k_D = 1.0$. Contrasting kinetic behavior is observed for **1a** (eq 1) versus **1c** (eq 2), with the roles of reactant for turnover and inhibitor reversed between the two systems. These disparate sets of observations can easily be misinterpreted as turnover for **1a** versus **1c** arising from different pathways, e.g., siliconate versus carbanion. However, analysis of the kinetics, KIEs, and DFT calculations of a wide range of potential intermediates (see SI) eventually leads to the conclusion that the two reagents elicit contrasting kinetics, selectivity ($3_{OSi}/4_{OSi}$), and KIEs, by biasing one of two extremes in a single overarching mechanism. Calculations employed the M06L/6-31+G* level of theory, which was selected from a range of other functionals and larger basis sets that were considered[63] (see SI), as it provided the best quantitative agreement with experiment. All calculations were performed in Gaussian09,[64] with THF solvation incorporated via a polarizable continuum model (PCM) single point at the same level of theory and with $T = 298$ K and pressure at 24.45 atm to achieve a 1 M standard state.[65] Kinetic isotope effects were computed using the Kinisot program.[66] Some of the TES- and TIPS-bearing structures required the "loose" settings during the geometry optimization, presumably because of the flat potential energy surface associated with the long Si–CF$_3$ bonds.

The calculations permitted several possible structure types (such as hexacoordinate silicon dianions) to be excluded from consideration and also revealed pronounced differences between intermediates based on TMS, TES, and TIPS, where the increasing steric bulk substantially destabilizes the pentacoordinate anions, Figure 6. Extensive calculations were conducted to test for direct nucleophilic reactivity of the pentacoordinate anions **B** and **D**. All calculations revealed that *direct* transfer of CF$_3$ from the silicon center to an electrophile requires concomitant inversion of the CF$_3$, with a prohibitively large barrier (>100 kcal mol^{-1}; in line with the barrier for inversion of the free CF$_3$ anion).[67] The pentacoordinate siliconate anions thus act as reservoirs, not active nucleophiles, liberating free (non-silicon-coordinated) CF$_3^-$ via dissociation. The transition state for addition of the CF$_3^-$ anion(oid) to the

ketone formally involves movement between a nonclassical hydrogen-bonded complex and the addition product, a process that occurs with low calculated barrier (7.5 kcal mol^{-1}) and well represents the process that occurs once the two species are in contact. The calculations support the known preference for deprotonation (k_{CH}) in the gas phase[68] and for addition (k_{CO}) once solvation is introduced, as observed experimentally for TMSCF$_3$ (**1a**). The loose addition transition state leads to a negligible ^{13}C KIE (carbonyl) for addition, while a large primary ^{2}H KIE is computed for C–H deprotonation. Relative rates computed from activation free energies suggest $\rho = 2.0$ for addition to acetophenones and a lower barrier for addition to 4-F-benzaldehyde (**13**) versus **2** ($\Delta\Delta G^{\ddagger}$ 2.6 kcal/mol; $k_{rel} = 81$). All of these computed values are in excellent agreement with experiment.

A general mechanism for the trifluoromethylation of ketones and aldehydes by R_3SiCF_3 reagents (**1**) in the presence of a catalytic quantity of initiator (M^+X^-) can thus be assembled, Figure 7. The one overarching mechanism, discussed below in the context of two extremes (Vi and Vii), rationalizes why the turnover rate (per M^+X^- initiator) for a given electrophile depends on the initial concentration (but not identity) of X$^-$, the identity (but not concentration) of M^+, the identity of the reagent (**1a–c**), and the electrophile/reagent ratio (**2/1**).

10. Mechanism Vi. In this regime, which describes reactions involving TMSCF$_3$ (**1a**), the dominant anion speciation is the bis(trifluoromethyl) siliconate (**D**),[32–34] generated in rapid equilibrium (K_3) with CF$_3^-$ (**E**)[36,38] and **1a**, as observed by NMR, Figure 4. The product-determining step (k_1) involves reaction of CF$_3^-$ (**E**) with the ketone (**2**) ($k_{CO} + k_{CH}$), and the reagent (**1a**) thus acts as a reversible inhibitor. The stronger the association of M^+ with CF$_3^-$ (see Section 13) and with the carbonyl oxygen, the faster the turnover rate: $Bu_4N^+ < [K(crypt-222)]^+ < [K(18-c-6)]^+ < K^+$. The initial concentration *ratios* of the reactant versus the reagent dictate the temporal evolution of the reaction. When $[2]_0/[1a]_0 = 1$, pseudo-zero-order kinetics are obtained, whereas when $[2]_0/[1a]_0 \geq 1$, the rate rises throughout the reaction, becoming very fast (asymptoting to $k_{-3}[D]$) in the final stages. The kinetics of trifluoromethylation of ketone **2** by TMSCF$_3$ (**1a**) can be satisfactorily simulated, Figure 8, using a truncated form of mechanism Vi that retains relationships

required for TOF modulation as the temporal concentration ratio $[2]_t/[1a]_t$ evolves.


$$k_1 K_3^{-1} = 7.1 \pm 1.2 \text{ s}^{-1}$$
$$k_3 \geq k_1 \geq 2000 \text{ M}^{-1}\text{s}^{-1}$$
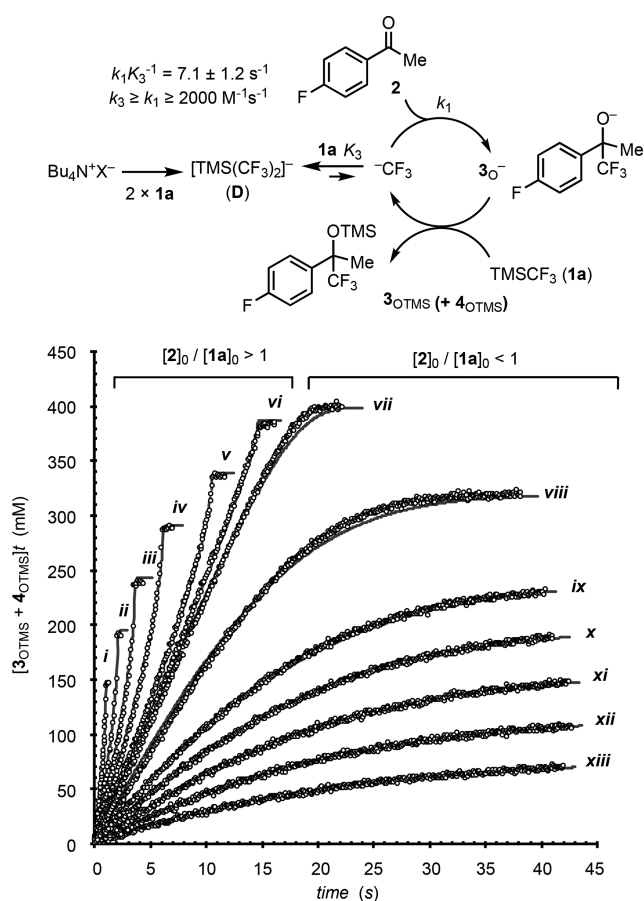
Figure 8. Simulation of experimental data (open circles, SF-IR; $[3_{OTMS} + 4_{OTMS}]_t$) based on simplified mechanism Vi, for reaction of ketone **2** with TMSCF$_3$ (**1a**), initiated by 3.6 mM TBAT (Bu$_4$N$^+$X$^-$). For $[2]_0/[1a]_0 > 1$, $[2]_0 = 0.40$ M and $[1a]_0 = 144, 192, 248, 288, 336, 384$ mM (i to vi). For $[2]_0/[1a]_0 < 1$, $[1a]_0 = 0.48$ M and $[2]_0 = 400, 320, 240, 200, 160, 120, 80$ mM (vii to xiii). Induction and turnover by **1a** are set to arbitrary high values. Fitted parameters (k_1, k_3, k_{-3}) are as indicated; $x_{EI} = 0$.[59]

11. Mechanism Vii. In this regime, which describes reactions involving TIPSCF$_3$ (**1c**), the dominant anion speciation is a combination of the product alkoxide (3_O^-), the enolate anion (4_O^-), and MX. Ketone **2** can reversibly H-bond (see **F** in Figure 7) with oxy-anions $3/4_O^-$, as observed by NMR, Figure 5, leading to inhibition (K_4).[69] When $[1c]_0/[2]_0 = 1$ pseudo-zero-order kinetics are observed; reactions in which $[1c]_0/[2]_0 > 1$ exhibit accelerating rate in the last stages of reaction. The more strongly bound M$^+$ to $[3/4_O^-]$, the slower the reaction with **1c**, leading to rates increasing in the series K$^+$ < [K(18-c-6)]$^+$ < Bu$_4$N$^+$ < [K(crypt-222)]$^+$, i.e., the opposite order to Vi. When the nonenolizable ketone 4-F-benzophenone **12** is employed, the kinetics show clean pseudo-first-order decay in **1c** (see SI), with no inhibition by **12** (i.e., mechanism Vii, where $K_4 = 0$, and eq 2, where $K_{i2} = 0$).

12. Competing Enolization. Also shown in Figure 7 is the generation of the enol ether (4_{OSi}) and CF$_3$H from ketone **2**, for which the selectivity ($4_{OSi}/3_{OSi}$) is dependent on M$^+$ and the reagent (**1a–c**), Table 1. The major pathway for

generation of 4_{OTMS} in mechanism Vi is via C–H deprotonation (k_{CH}) with an attendant large primary ^{2}H-KIE.[70,71] In contrast, for mechanism Vii, the significant concentration of $[3/4_O^-]$ allows keto–enol equilibrium (p$K_{enol} \approx 8$)[72] in **2** to be approached, with attendant intermolecular scrambling of ^{2}H between ketone methyl groups. Deprotonation (k_{OH}) of the enol (2_{enol}) is predicted (DFT) to be of very low barrier and thus proceed with a negligible ^{2}H-KIE.[70] Despite their different origins (k_{CH} versus k_{OH}) mechanisms Vi and Vii both lead to $4_{OSi}/3_{OSi}$ ratios that are independent of the concentration of reactants (**1**, **2**) and constant throughout the reaction, Figure 2.

13. Cation–CF$_3$ Interactions. The interactions between the CF$_3^-$ anion (free and Si-bound) and the counter-cations K$^+$ and Me$_4$N$^+$ (as a model for Bu$_4$N$^+$) were explored computationally, with multidentate CF$_3$ interactions found to be favored, e.g. Figure 9; see SI for details.
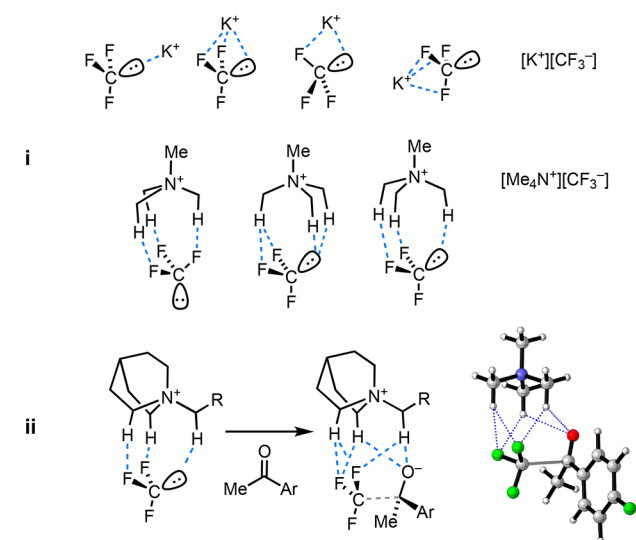
Figure 9. Cation binding to free CF$_3$ anion: (i) various modes of binding of K$^+$ and Me$_4$N$^+$ cations; (ii) concept (schematic) for enantioselective addition beneath the quinuclidinium core of a cinchonidinium initiator. Inset: Structure of TS for addition of [CF$_3^-$][Me$_4$N$^+$] to **2** (see SI) with H-bonding interactions to developing alkoxide anion.

The *indirect* transfer of CF$_3$ from reagent **1a** to the ketone/aldehyde, i.e., via a silicon-free carbanion **E**, has implications for the mode by which enantioselective catalysis can be achieved using chiral ammonium initiators, e.g., cinchonidinium salts. The CF$_3^-$ anion binding modes found computationally for Me$_4$N$^+$ (Figure 9i) show how an ammonium cation might simultaneously interact with a CF$_3^-$ anion and control a developing alkoxide anion, Figure 9ii. Mechanism Vi contrasts most,[16d,e,31] but not all,[16f] prior interpretations, where mechanisms II/III (Scheme 2) involving CF$_3$-siliconates bearing the initiating (**C**) or propagating (**B**) anion, are proposed to play key roles in the enantioselective trifluoromethylation step.

14. Broader Mechanistic Aspects. The mechanistic features elucidated in the current study extend beyond carbonyl trifluoromethylation. A number of corollaries follow for generic anion-initiated trifluoromethylation of an electrophile (**E**) by **1a**, or deprotonation (R–H),[73] via pathways analogous to mechanism Vi, and where $[E, \text{R–H}]_0 \gg$

$[M^+X^-]_0$. Thus, the initiator (M^+X^-) affects the rate of reaction in a number of ways. $[X^-]_0$ sets the initial concentration of the siliconate $([\mathbf{D}]_0 = (1 - x_{EI})[X^-]_0)$,[60] which, in the absence of endogenous inhibitors, is essentially constant throughout the reaction. The insurmountable barrier for CF_3 inversion[67] means that, independent of the identity of the electrophile, E, or proton donor, R−H, the siliconate is unable to effect direct anionic trifluoromethyl transfer, Figure 10i. In all cases, the reaction must proceed via a dissociative
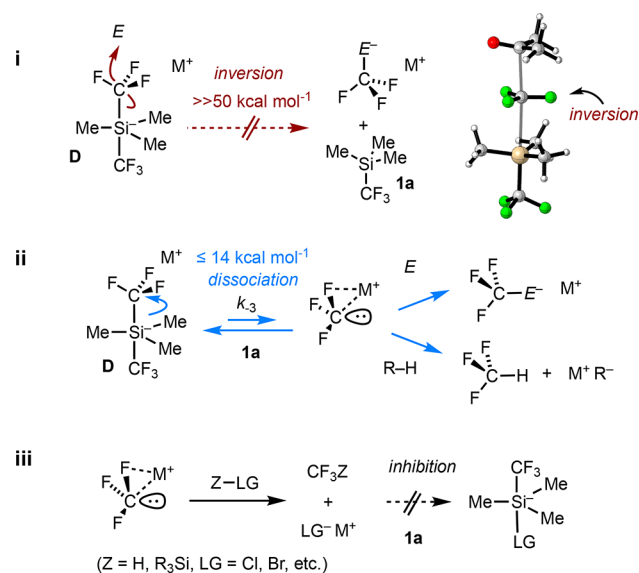
Figure 10. Generic reactivity of siliconate $\mathbf{D}$ toward electrophiles (E), carbon acids (R−H), and inhibitors (Z−LG). (i) *Direct* CF_3 transfer from $\mathbf{D}$ is strongly disfavored. Inset: TS for CF_3 transfer to acetone; see SI. (ii) *Dissociative* CF_3 transfer, without CF_3 inversion. (iii) Termination of the anionic chain reaction by traces of exogenous inhibitor(s) or substrates that generate an unreactive anion, LG⁻.

pathway, Figure 10ii, in which M^+ plays a key role: the stronger the association of M^+ with CF_3, the more favorable k_{-3}. In contrast, efficient regeneration of the siliconate (k_2, Figure 7) is favored by weaker interactions between M^+ and the anionic coproduct from trifluoromethyl transfer (CF_3-E^-; R⁻; or products thereof). When the anion is unable to react with **1a**, stoichiometric initiation by $[M^+X^-]$ is required.[14−26]

15. Exogenous Inhibition. Trifluoromethylations initiated by low concentrations of (M^+X^-) are highly sensitive to traces of exogenous inhibitor(s). Species that generate an anion (LG⁻) of insufficient reactivity toward **1a** to propagate will terminate the anionic chain reaction, Figure 10iii. In a series of control experiments, additives of the form Z-LG, (Z = H, R_3Si, LG = Cl, Br) were found to function as powerful inhibitors for the anion-initiated reaction of **2** with **1a**. For example, the trifluoromethylation of **2** (0.4 M) initiated by 150 μM TBAT ceases immediately on addition of 150 μM TMSCl; see SI. Slower-onset irreversible inhibition is effected by the more hindered TIPSCl, which also inhibits the reaction of TIPSCF₃ (**1c**). Competing consumption of **1a** is effected by other species in low concentrations, including CCl_4 (Cl transfer),[74] Cl_3CH (deprotonation/Cl transfer),[73b] and TMS−OH (deprotonation), but without significant chain termination. There was no detectable inhibition by dichloroethane (DCE), CH_2Cl_2,[73b] TMS-O-TMS, Ph_3SiF, Me_3SiCF_2H, or MeCN.[73c]

In our experience, a diverse range of inhibitors and competitors (e.g., CCl_4 and $CHCl_3$) are present, in low concentrations and variable proportions, in commercial samples of TMSCF₃ (**1a**). This leads to substantial differences in reaction outcome, depending on the supplier. For example, comparison of the reaction of **2** (0.40 M) with five samples of distilled **1a** (0.48 M) revealed that the concentration of initiator (TBAT, KOPh) required to effect >99% conversion of **2** ranged from 30 μM to 2.0 mM (0.0075 to 0.5 mol %); see SI.

A major difference found between reactions involving reagent **1a** versus **1b,c** is the impact of the persistent radical, TEMPO, which powerfully inhibits reactions involving **1a**, Scheme 4A. The difference in behavior toward TEMPO cannot arise from oxidation of the CF_3 anion (E), as this is a common intermediate to all three reagents (**1a−c**), and the partitioning of E between reaction with the ketone (**2**) versus TEMPO will be constant across the series, i.e., *independent* of the provenance of the carbanion E. Since the major difference between reagents **1a** and **1c** under the conditions of the reaction is the dominant anion speciation ($\mathbf{D}$; mechanism Vi, **1a**, versus alkoxides $3_O^-/4_O^-$, mechanism Vii, **1c**), this suggests that reaction of siliconate $\mathbf{D}$ with TEMPO is responsible for the inhibition. We were unable to identify any products *in situ* or by quenching, arising from TEMPO under the standard reaction conditions; see SI. While siliconates of type $\mathbf{D}$ are also generated from **1b** and **1c**, they (a) are only present at low concentration or as transient species, thus reducing their net rate of reaction with TEMPO, and (b) may be more resistant to reaction with TEMPO due to their greater steric bulk.

■ CONCLUSIONS

The trifluoromethylation of ketones and aldehydes by TMSCF₃ (**1a**), initiated by catalytic fluoride ion, has been employed in synthesis for three decades.[17] Previous mechanistic work has focused on stoichiometric reactions of R_3SiCF_3 (**1a,c**) with anions at low temperatures, generating unstable trifluoromethyl siliconates ($\mathbf{C}$, $\mathbf{D}$)[32−34] and carbanion(oids) (E),[36−38] depending on conditions. Which of these two pathways is followed in catalytic reactions at ambient temperature has been a long-standing mechanistic dichotomy.[30] A variable-ratio stopped-flow NMR/IR approach (Figure 3) has been developed to facilitate time- and material-efficient analysis of a wide range of initiator (M^+X^-) and reactant concentrations. Change of reagent from TMSCF₃ (**1a**) to TIPSCF₃ (**1c**) has a profound impact on the reaction. For example, the conversion of 4-F-acetophenone (**2**, 0.4 M) to 3_{OTMS} by equimolar **1a** in THF at ambient temperature takes <125 ms to complete using 0.1 mol % KOPh initiator and generates <2% of silylenol ether 4_{OTMS}, whereas with TIPSCF₃ (**1c**) and 3.75 mol % KOPh, the reaction proceeds to just 60% conversion in 16 h and generates 50% 4_{OTIPS}. The rates of reaction are strongly affected by traces of inhibitors present in the reagents (**1**), especially at the low concentrations of initiator (M^+X^-) employed for the fastest reacting systems; see eqs 1 and 2.[59,60] Nonetheless, while these render misleading initial rate data, study of the full reaction time-course, e.g., Figure 8, provides a coherent kinetics analysis.

A unified mechanism (V) for the reaction of R_3SiCF_3 reagents (**1a−c**) with ketones and aldehydes under conditions of catalytic anionic initiator (M^+X^-) is presented in Figure 7. The work confirms that the carbanion[36−38] mechanism prevails

under conditions of application (Scheme 1). Mechanism V allows a number of initially confusing observations to be rationalized. The main difference between use of TMSCF$_3$ (**1a**) versus TIPSCF$_3$ (**1c**) reagents is an inversion in the major anion speciation in the overall anionic chain reaction. This inversion leads to opposing influences of electrophile and silicon reagent (mechanisms V*i* and V*ii*) and to keto−enol equilibration (**2**/**2**$_{enol}$) with **1c** (V*ii*). When TBAT is used as initiator,[75] TESCF$_3$ (**1b**) effects the most rapid trifluoromethylation in the series **1a**−**c**. The increased steric bulk in **1b** reduces reagent inhibition (K_3) relative to **1a**, without the substantial kinetic penalty in k_2 experienced by **1c**. These factors shift the reaction with **1b** closer to an "ideal" catalytic cycle in which the intermediates are all connected by low TS barriers, with reduced off-cycle speciation. A consequence of adding TMSCF$_3$ (**1a**) to TESCF$_3$ (**1b**) is therefore to strongly inhibit turnover of **1b** until all of **1a** has been consumed, Figure 1.

The overarching mechanism (V, Figure 7) for anion-initiated reactions of R$_3$SiCF$_3$ (**1**) with ketones and aldehydes should prove of utility in their application in synthesis. For example, in the context of the design and analysis of enantioselective trifluoromethylation processes,[16,29,30a,31] mechanism V shows that control must be achieved by the CF$_3^-$/[M]$^+$ ion pair, Figure 9ii, and not by a siliconate intermediate. Moreover, the key mechanistic features of the anion-initiated reactions of **1** with carbonyl compounds (Figure 7) translate to reactions of **1** with other electrophiles (E)[29−31] and proton donors (R−H to generate R$^-$),[73] Figure 10. Thus, all processes in which siliconate **D** or analogous species formally acts as a nucleophilic or basic source of CF$_3$ must proceed via a dissociative pathway (Figure 10ii). Siliconate **D** is inherently unstable and decomposes at ambient temperature to generate, *inter alia*, complex perfluorocarbanions.[34,38a] The rate of anionic chain transfer, as dictated by the reactivity of the electrophile (E)[29−31] or carbon acid (R−H)[73] toward CF$_3^-$, as well as the presence of species able to attenuate decomposition (e.g., via CF$_2$ capture, **4**$_{OSi}$ →**10**, Scheme 3), controls the formal lifetime of **D** and in turn the minimum loading of initiator (M$^+$X$^-$) that will be required to achieve complete conversion of substrate. Moreover, traces of exogenous inhibitor(s) (e.g., Z−LG, Figure 10iii) ubiquitous in R$_3$SiCF$_3$ reagents (**1**) act to reduce the net active anion in the chain reaction, again increasing the requisite loading of initiator (M$^+$X$^-$). Compounds employed in synthetic routes to reagents **1a**−**c**, e.g., TMSCl and TIPSCl,[11] function as powerful inhibitors. However, the identity and effect of the inhibitors in reagents **1a**−**c** vary substantially from batch to batch and between commercial suppliers (see SI). Electrophiles or carbon acids (R−H) that react with CF$_3^-$ to ultimately generate an anion of inherently low reactivity toward **1** require a stoichiometric initiator to proceed to completion.[14−26]

ASSOCIATED CONTENT

ⓢ Supporting Information

The Supporting Information is available free of charge on the ACS Publications website at DOI: 10.1021/jacs.8b06777.

> Additional discussion, experimental procedures, further
> kinetic data and analysis, characterization data, and
> NMR spectra (PDF)

AUTHOR INFORMATION

Corresponding Author
*Guy.lloyd-jones@ed.ac.uk
ORCID ⊙
Andrew G. Leach: 0000-0003-1325-8273
Guy C. Lloyd-Jones: 0000-0003-2128-6864
Author Contributions
⊥C. P. Johnston and T. H. West contributed equally to this work.
Notes
The authors declare no competing financial interest.

REFERENCES

(1) Selected reviews: (a) Purser, S.; Moore, P. R.; Swallow, S.; Gouverneur, V. *Chem. Soc. Rev.* **2008**, *37*, 320−330. (b) Gillis, E. P.; Eastman, K. J.; Hill, M. D.; Donnelly, D. J.; Meanwell, N. A. *J. Med. Chem.* **2015**, *58*, 8315−8359. (c) Zhou, Y.; Wang, J.; Gu, Z.; Wang, S.; Zhu, W.; Aceña, J. L.; Soloshonok, V. A.; Izawa, K.; Liu, H. *Chem. Rev.* **2016**, *116*, 422−518.

(2) Selected recent reviews: (a) Fujiwara, T.; O'Hagan, D. *J. Fluorine Chem.* **2014**, *167*, 16−29. (b) Jeschke, P. *Pest Manage. Sci.* **2010**, *66*, 10−27.

(3) Babudri, F.; Farinola, G. M.; Naso, F.; Ragni, R. *Chem. Commun.* **2007**, 1003−1022.

(4) Berger, R.; Resnati, G.; Metrangolo, P.; Weber, E.; Hulliger, J. *Chem. Soc. Rev.* **2011**, *40*, 3496−3508.

(5) *Fluorinated Polymers* (Vols. 1 and 2); Ameduri, B.; Sawada, H., Eds.; Royal Society of Chemistry: Cambridge, U.K., 2017.

(6) Ni, C.; Hu, J. *Chem. Soc. Rev.* **2016**, *45*, 5441−5454.

(7) Vincent, J. M. *Top. Curr. Chem.* **2011**, *308*, 153−174.

(8) Langlois, B. R.; Billard, T.; Roussel, S. *J. Fluorine Chem.* **2005**, *126*, 173−179.

(9) See for example: (a) Zhang, Y.; Fujiu, M.; Serizawa, H.; Mikami, K. *J. Fluorine Chem.* **2013**, *156*, 367−371. (b) Musio, B.; Gala, E.; Ley, S. V. *ACS Sustainable Chem. Eng.* **2018**, *6*, 1489−1495.

(10) (a) Geri, J. B.; Szymczak, N. K. *J. Am. Chem. Soc.* **2017**, *139*, 9811−9814. (b) Geri, J. B.; Wade Wolfe, M. M.; Szymczak, N. K. *Angew. Chem., Int. Ed.* **2018**, *57*, 1381−1385.

(11) (a) Ruppert, I.; Schlich, K.; Volbach, W.; Die Ersten. *Tetrahedron Lett.* **1984**, *25*, 2195−2198. (b) Ramaiah, P.; Krishnamurti, R.; Prakash, G. K. S. *Org. Synth.* **1995**, *72*, 232−236. (c) Prakash, G. K. S.; Jog, P. V.; Batamack, P. T. D.; Olah, G. A. *Science* **2012**, *338*, 1324−1327. (d) Pawelke, G. *J. Fluorine Chem.* **1989**, *42*, 429−433. (e) Eaborn, C.; Griffiths, R. W.; Pidcock, A. *J. Organomet. Chem.* **1982**, *225*, 331−341.

(12) (a) Kruse, A.; Siegemund, G.; Schumann, A.; Ruppert, I. A process for the production of perfluoroalkyl compounds, and the pentafluoroethyl-trimethylsilane. German Pat. DE3805534, 1989; priority date February 23, 1988.

(13) (a) Prakash, G. K. S.; Krishnamurti, R.; Olah, G. A. *J. Am. Chem. Soc.* **1989**, *111*, 393−395. See also: (b) Stahly, G. P.; Bell, D.

R. *J. Org. Chem.* **1989**, *54*, 2873−2877. (c) Dubuffet, T.; Sauvêtre, R.; Normant, J. F. *Tetrahedron Lett.* **1988**, *29*, 5923−5924. For analogous fluoride-initiated nucleophilic transfer of CF$_2$H, see: (d) Chen, D.; Ni, C.; Zhao, Y.; Cai, X.; Li, X.; Xiao, P.; Hu, J. *Angew. Chem., Int. Ed.* **2016**, *55*, 12632−12636.

(14) (a) Prakash, G. K. S.; Yudin, A. K. *Chem. Rev.* **1997**, *97*, 757−786. (b) Singh, R. P.; Shreeve, J. M. *Tetrahedron* **2000**, *56*, 7613−7632. (c) Gawronski, J.; Wascinska, N.; Gajewy, J. *Chem. Rev.* **2008**, *108*, 5227−5252.

(15) (a) Singh, R. P.; Cao, G.; Kirchmeier, R. L.; Shreeve, J. M. *J. Org. Chem.* **1999**, *64*, 2873−2876. (b) Krishnamturi, R.; Bellew, D. R.; Prakash, G. K. S. *J. Org. Chem.* **1991**, *56*, 984−989. (c) Prakash, G. K. S.; Panja, C.; Vaghoo, H.; Surampudi, V.; Kultyshev, R.; Mandal, M.; Rasul, G.; Mathew, T.; Olah, G. A. *J. Org. Chem.* **2006**, *71*, 6806−6813.

(16) (a) Mizuta, S.; Shibata, N.; Akiti, S.; Fujimoto, H.; Nakamura, S.; Toru, T. *Org. Lett.* **2007**, *9*, 3707−3710. (b) Mizuta, S.; Shibata, N.; Hibino, M.; Nagano, S.; Nakamura, S.; Toru, T. *Tetrahedron* **2007**, *63*, 8521−8528. (c) Nagao, H.; Kawano, Y.; Mukaiyama, T. *Bull. Chem. Soc. Jpn.* **2007**, *80*, 2406−2412. (d) Hu, X.; Wang, J.; Wei, L.; Lin, L.; Liu, X.; Feng, X. *Tetrahedron Lett.* **2009**, *50*, 4378−4380. (e) Zhao, H.; Qin, B.; Liu, X.; Feng, X. *Tetrahedron* **2007**, *63*, 2682−2686. (f) Caron, S.; Do, N. M.; Arpin, P.; Larivee, A. *Synthesis* **2003**, *2003*, 1693−1698. (g) Kawai, H.; Mizuta, S.; Tokunaga, E.; Shibata, N. *J. Fluorine Chem.* **2013**, *152*, 46−50. (h) Okusu, S.; Hirano, K.; Yasuda, Y.; Tokunaga, E.; Shibata, N. *RSC Adv.* **2016**, *6*, 82716−82720.

(17) For example, a substructure search on 14/06/2018 for the addition of TMSCF$_3$ (**1a**, exact reagent) to C≡O (any carbonyl) → C(OA)-CF$_3$ (A = any atom) using Reaxys/SciFinder gave 434/450 primary research papers and 631/811 patents.

(18) Dilman, A. D.; Levin, V. V. *Eur. J. Org. Chem.* **2011**, *2011*, 831−841.

(19) (a) Jin, G.; Zhang, X.; Fu, D.; Dai, W.; Cao, S. *Tetrahedron* **2015**, *71*, 7892−7899. (b) Ono, T. *J. Fluorine Chem.* **2017**, *196*, 128−134.

(20) (a) Furin, G. G.; Bardin, V. V. *J. Fluorine Chem.* **1991**, *54*, 241−241. (b) Bardin, V. V.; Kolomeitsev, A. A.; Furin, G. G.; Yagupol'skii, Y. L. *Bull. Acad. Sci. USSR, Div. Chem. Sci.* **1990**, *39*, 1539−1539.

(21) (a) Kolomeitsev, A. A.; Movchun, V. N.; Kondratenko, N. V.; Yagupolski, Y. L. *Synthesis* **1990**, *1990*, 1151−1152. (b) Kowalczyk, R.; Edmunds, A. J.; Hall, R. G.; Bolm, C. *Org. Lett.* **2011**, *13*, 768−771. (c) Gouault-Bironneau, S.; Timoshenko, V. M.; Grellepois, F.; Portella, C. *J. Fluorine Chem.* **2012**, *134*, 164−171. (d) Timoshenko, V. M.; Portella, C. *J. Fluorine Chem.* **2009**, *130*, 586−590. (e) Yagupolskii, L. M.; Matsnev, A. V.; Orlova, R. K.; Deryabkin, B. G.; Yagupolskii, Y. L. *J. Fluorine Chem.* **2008**, *129*, 131−136.

(22) (a) Billard, T.; Langlois, B. R.; Large, S. *Phosphorus, Sulfur Silicon Relat. Elem.* **1998**, *136*, 521−524. (b) Tyrra, W.; Naumann, D.; Yagupolskii, Y. L. *J. Fluorine Chem.* **2003**, *123*, 183−187.

(23) (a) Tworowska, I.; Dabkowski, W.; Michalski, J. *Angew. Chem., Int. Ed.* **2001**, *40*, 2898−2900. (b) Pane, P.; Naumann, D.; Hoge, B. *J. Fluorine Chem.* **2001**, *112*, 283−286. (c) Murphy-Jolly, M. B.; Lewis, L. C.; Caffyn, A. J. M. *Chem. Commun.* **2005**, 4479−4480.

(24) (a) Molander, G. A.; Hoag, B. P. *Organometallics* **2003**, *22*, 3313−3315. (b) Kolomeitsev, A. A.; Kadyrov, A. A.; Szczepkowska-Sztolcman, J.; Milewska, M.; Koroniak, H.; Bissky, G.; Barten, J. A.; Röschenthaler, G.-V. *Tetrahedron Lett.* **2003**, *44*, 8273−8277.

(25) Matousek, V.; Pietrasiak, E.; Schwenk, R.; Togni, A. *J. Org. Chem.* **2013**, *78*, 6763−6768.

(26) Tyrra, W.; Naumann, D.; Kirij, N. V.; Kolomeitsev, A. A.; Yagupolskii, Y. L. *J. Chem. Soc., Dalton Trans.* **1999**, 657−658.

(27) (a) Prakash, G. K. S.; Krishnamoorthy, S.; Kar, S.; Olah, G. A. *J. Fluorine Chem.* **2015**, *180*, 186−191. (b) Hashimoto, R.; Iida, T.; Aikawa, K.; Ito, S.; Mikami, K. *Chem. - Eur. J.* **2014**, *20*, 2750−2754. (c) Ito, S.; Kato, N.; Mikami, K. *Chem. Commun.* **2017**, *53*, 5546−5548.

(28) Ni, C.; Hu, J. *Synthesis* **2014**, *46*, 842−863.

(29) (a) Liu, X.; Xu, C.; Wang, M.; Liu, Q. *Chem. Rev.* **2015**, *115*, 683−730. (b) Takeshi Komiyama, T.; Minami, Y.; Hiyama, T. *ACS Catal.* **2017**, *7*, 631−651.

(30) (a) Denmark, S. E.; Buetner, G. L. *Angew. Chem., Int. Ed.* **2008**, *47*, 1560−1638. (b) Reich, H. J. Mechanism of C-Si Bond Cleavage Using Lewis Bases (n→σ*). In *Lewis Base Catalysis in Organic Synthesis*, 1st ed.; Vedejs, E.; Denmark, S. E., Eds.; Wiley VCH: Weinheim, Germany, 2016; Vol. 1, pp 251−253.

(31) For leading references see: (a) Yang, X.; Wu, T.; Phipps, R. J.; Toste, F. D. *Chem. Rev.* **2015**, *115*, 826−870. (b) Shibata, N.; Mizuta, S.; Kawai, H. *Tetrahedron: Asymmetry* **2008**, *19*, 2633−2644.

(32) Maggiarosa, N.; Tyrra, W.; Naumann, D.; Kirij, N. V.; Yagupolskii, Y. L. *Angew. Chem., Int. Ed.* **1999**, *38*, 2252−2253.

(33) Kolomeitsev, A.; Bissky, G.; Lork, E.; Movchun, V.; Rusanov, E.; Kirsch, P.; Röschenthaler, G.-V. *Chem. Commun.* **1999**, 1017−1018.

(34) Tyrra, W.; Kremlev, M. M.; Naumann, D.; Scherer, H.; Schmidt, H.; Hoge, B.; Pantenburg, I.; Yagupolskii, Y. L. *Chem. - Eur. J.* **2005**, *11*, 6514−6518.

(35) Kotun, S. P.; Anderson, J. D. O.; DesMarteau, D. D. *J. Org. Chem.* **1992**, *57*, 1124−1131.

(36) Prakash, G. K. S.; Wang, F.; Zhang, Z.; Haiges, R.; Rahm, M.; Christe, K. O.; Mathew, T.; Olah, G. A. *Angew. Chem., Int. Ed.* **2014**, *53*, 11575−11578.

(37) Santschi, N.; Gilmour, R. *Angew. Chem., Int. Ed.* **2014**, *53*, 11414−11415.

(38) (a) Lishchynskyi, A.; Miloserdov, F. M.; Martin, E.; Benet-Buchholz, J.; Escudero-Adán, E. C.; Konovalov, A. I.; Grushin, V. V. *Angew. Chem., Int. Ed.* **2015**, *54*, 15289−15293. (b) Miloserdov, F. M.; Konovalov, A. I.; Martin, E.; Benet-Buchholz, J.; Escudero-Adán, E. C.; Lishchynskyi, A.; Grushin, V. V. *Helv. Chim. Acta* **2017**, *100*, e1700032. (c) Harlow, R. L.; Benet-Buchholz, J.; Miloserdov, F. M.; Konovalov, A. I.; Marshall, W. J.; Martin, E.; Benet-Buchholz, J.; Escudero-Adán, E. C.; Martin, E.; Lishchynskyi, A.; Grushin, V. V. *Helv. Chim. Acta* **2018**, *101*, e1800015.

(39) The X-ray structural analysis of E (ref 38a) was challenged: Becker, S.; Müller, P. *Chem. - Eur. J.* **2017**, *23*, 7081−7086. The original interpretation was comprehensively defended; see ref 38c.

(40) The CF$_3$H contained traces of CF$_3$D (0.1% ^{19}F NMR) likely from adventitious DOH/D$_2$O in the d_8-THF.

(41) Song, X.; Chang, J.; Zhu, D.; Li, J.; Xu, C.; Liu, Q.; Wang, M. *Org. Lett.* **2015**, *17*, 1712−1715.

(42) Song, X.; Xu, C.; Du, D.; Zhao, Z.; Zhu, D.; Wang, M. *Org. Lett.* **2017**, *19*, 6542−6545.

(43) Pilcher, A. S.; DeShong, P. *J. Org. Chem.* **1996**, *61*, 6901−6905.

(44) Water may be liberated from the NMR tube surface, the reagents (**1a**, **2**; freshly distilled), the TBAT (anhydrous solid; THF solutions prepared and stored in a glovebox), or the THF (~8 ppm H$_2$O, Karl Fischer titration).

(45) Turnover rates were affected only by the impact on TMSCF$_3$/ketone ratio resulting from the rapid prior consumption of TMSCF$_3$ by the H$_2$O.

(46) For a review of CF$_3$ transfer involving CF$_3$ radicals, see: Studer, A. *Angew. Chem., Int. Ed.* **2012**, *51*, 8950−8958.

(47) For an example of CF$_3$ radical character transfer from TMSCF$_3$ via AgCF$_3$ intermediates, see: Ye, Y.; Lee, S. H.; Sanford, M. S. *Org. Lett.* **2011**, *13*, 5464−5467 and references therein.

(48) Competing 1,4- and 1,6-addition to the aryl ring are characteristic of SET-type mechanisms for nucleophile addition to benzophenones; see: Holm, T.; Crossland, I. *Acta Chem. Scand.* **1971**, *25*, 59−69 and references therein.

(49) A near-continuum sequential SET pathway is possible; see e.g.: Eisch, J. J. *Res. Chem. Intermed.* **1996**, *22*, 145−187.

(50) (a) Newcombe, M.; Johnson, C. C.; Manek, M. B.; Varick, T. R. *J. Am. Chem. Soc.* **1992**, *114*, 10915−10921. (b) Miyazoe, H.; Yamago, S.; Yoshida, J. *Angew. Chem., Int. Ed.* **2000**, *39*, 3669−3671.

(51) Biphenyl is significantly more stabilizing for radical pathways than 4-fluorophenyl ($\sigma C^\bullet$, +0.46 and −0.06 respectively), see: Creary, X. *Acc. Chem. Res.* **2006**, *39*, 761−771.

(52) For example, BuN$^+$X$^-$ where X$^-$ = Ph$_3$SiF$_2$$^-$, F$^-$, HO$^-$, PhO$^-$, AcO$^-$, and $3_O$$^-$, behaved identically within experimental error. However when X$^-$ was less nucleophilic, e.g., BzO$^-$, or 3,5-(CF$_3$)C$_6$H$_3$O$^-$, significant induction periods were evident. Induction periods were extreme with KOC(CF$_3$)$_3$.

(53) Luo, G.; Luo, Y.; Qu, J. *New J. Chem.* **2013**, *37*, 3274−3280.

(54) Control experiments confirmed that TBAT induces negligible H/D exchange between **2** and D$_3$-**2** over the reaction period, whereas 3_{OK} induces complete scrambling in under 95 s.

(55) For examples of mechanical variable ratio mixing for stopped-flow kinetics see: Goez, M. *J. Phys. E: Sci. Instrum.* **1988**, *21*, 440−442 and references therein.

(56) For recent developments see: (a) Dunn, A. L.; Landis, C. R. *Magn. Reson. Chem.* **2017**, *55*, 329−336. (b) Thomas, A. A.; Denmark, S. E.; Ernest, L. Eliel, a Physical Organic Chemist with the Right Tool for the Job: Rapid Injection Nuclear Magnetic Resonance. In *Stereochemistry and Global Connectivity: The Legacy of Ernest L. Eliel*, Cheng, H. N., Ed.; American Chemical Society: Washington DC, 2017; Vol. 2, pp 105−134.

(57) Cox, P. A.; Reid, M.; Leach, A. G.; Campbell, A. D.; King, E. J.; Lloyd-Jones, G. C. *J. Am. Chem. Soc.* **2017**, *139*, 13156−13165.

(58) Foley, D. A.; Bez, E.; Codina, A.; Colson, K. L.; Fey, M.; Krull, R.; Piroli, D.; Zell, M. T.; Marquez, B. L. *Anal. Chem.* **2014**, *86*, 12008−12013.

(59) Plots of initial rate versus [TBAT] for reaction of **2** and **13** with **1a** both have a nonzero *x*-axis intercept (0.03 mM) with curvature evident at low [TBAT] concentrations, suggesting the inhibitor(s) are present at <0.02% **1a**, in the specific batches of commercial reagents that were employed; see SI.

(60) In eqs 1 and 2 and elsewhere, $(1 - x_{EI})$ represents the mole fraction of active anion relative to total anion [M$^+$X$^-$]$_0$. Based on a 1:1 inhibition mode, $x_{EI} = (K_{EI}[I]/(1 + K_{EI}[I]))$ with [I]$_0$ = x_i[**1**]$_0$, where x_i = mole fraction inhibitor in reagent **1**. Experimental data (see SI) suggest K_{EI} is substantially greater with **1c**.

(61) This contrasts with the borazine systems recently developed by Szymczak (see ref 10), where addition of KBARF profoundly accelerates CF$_3$-transfer rates.

(62) Simulations were conducted using the three-spin parametrization in WNDNMR, with the rates and frequencies as indicated in Figure 4 ($k_{ex} = 2k_{-ex}$; where k_{-ex} is the apparent ^{19}F nuclei exchange rate through reassociation). The fraction of CF$_3$ present as **E** was arbitrarily set to 0.1%, with the remaining 99.9% partitioned between **D** and **1a** as required to fit. The chemical shift of CF$_3$[M] is reported as δ_F −18.7 ppm (see ref 38, and −17.2 ppm, see ref 36), depending on the identity of [M].

(63) Hariharan, P. C.; Pople, J. A. *Theor. Chim. Acta* **1973**, *28*, 213−222.

(64) Frisch, M. J.; Trucks, G. W.; Schlegel, H. B.; Scuseria, G. E.; Robb, M. A.; Cheeseman, J. R.; Scalmani, G.; Barone, V.; Mennucci, B.; Petersson, G. A.; Nakatsuji, H.; Caricato, M.; Li, X.; Hratchian, H. P.; Izmaylov, A. F.; Bloino, J.; Zheng, G.; Sonnenberg, J. L.; Hada, M.; Ehara, M.; Toyota, K.; Fukuda, R.; Hasegawa, J.; Ishida, M.; Nakajima, T.; Honda, Y.; Kitao, O.; Nakai, H.; Vreven, T.; Montgomery, J. A., Jr.; Peralta, J. E.; Ogliaro, F.; Bearpark, M.; Heyd, J. J.; Brothers, E.; Kudin, K. N.; Staroverov, V. N.; Kobayashi, R.; Normand, J.; Raghavachari, K.; Rendell, A.; Burant, J. C.; Iyengar, S. S.; Tomasi, J.; Cossi, M.; Rega, N.; Millam, J. M.; Klene, M.; Knox, J. E.; Cross, J. B.; Bakken, V.; Adamo, C.; Jaramillo, J.; Gomperts, R.; Stratmann, R. E.; Yazyev, O.; Austin, A. J.; Cammi, R.; Pomelli, C.; Ochterski, J. W.; Martin, R. L.; Morokuma, K.; Zakrzewski, V. G.; Voth, G. A.; Salvador, P.; Dannenberg, J. J.; Dapprich, S.; Daniels, A. D.; Farkas, Ö.; Foresman, J. B.; Ortiz, J. V.; Cioslowski, J.; Fox, D. J. *Gaussian 09*; Gaussian, Inc.: Wallingford, CT, 2009.

(65) (a) Zhao, Y.; Truhlar, D. G. *Theor. Chem. Acc.* **2008**, *120*, 215−241. (b) Zhao, Y.; Truhlar, D. G. *Acc. Chem. Res.* **2008**, *41*, 157−167. (c) Tomasi, J.; Mennucci, B.; Cammi, R. *Chem. Rev.* **2005**, *105*, 2999−3094.

(66) (a) Brown, S. B.; Dewar, M. J. S.; Ford, G. P.; Nelson, D. J.; Rzepa, H. S. *J. Am. Chem. Soc.* **1978**, *100*, 7832−7836. (b) Dewar, M. J. S.; Olivella, S.; Rzepa, H. S. *J. Am. Chem. Soc.* **1978**, *100*, 5650−5659. (c) Rzepa, H. S. *KINISOT. A basic program to calculate kinetic isotope effects using normal coordinate analysis of transition state and reactants*; http://doi.org/10.5281/zenodo.19272, 2015. (d) Paton, R. S. *Kinisot*: v 1.0.0 public API for Kinisot.py. http://doi.org/10.5281/zenodo.60082, 2016.

(67) Han, H.; Alday, B.; Shuman, N. S.; Wiens, J. P.; Troe, J.; Viggiano, A. A.; Guo, H. *Phys. Chem. Chem. Phys.* **2016**, *18*, 31064−31071.

(68) McDonald, R. N.; Chowdhury, A. K. *J. Am. Chem. Soc.* **1983**, *105*, 7267−7271.

(69) For a range of anion−ketone interactions, including H-bonded adducts and aldolate products, see: Kolonko, K. J.; Reich, H. J. *J. Am. Chem. Soc.* **2008**, *130*, 9668−9669. The lowest energy of these was an enolate-ketone H-bonded adduct (**F**).

(70) Thibblin, A.; Jencks, W. P. *J. Am. Chem. Soc.* **1979**, *101*, 4963−4973.

(71) The ^{2}H-KIE for α-C−H deprotonation of d_3-**2** by LDA.LiOR is k_H/k_D = 6.3; with (LDA)$_2$ it is 1.7: Kolonko, K. J.; Wherrit, D. J.; Reich, H. J. *J. Am. Chem. Soc.* **2011**, *133*, 16774−16777.

(72) Chiang, Y.; Kresge, A. J.; Wirz, J. *J. Am. Chem. Soc.* **1984**, *106*, 6392−6395.

(73) (a) Sasaki, M.; Kondo, Y. *Org. Lett.* **2015**, *17*, 848−851. (b) Behr, J.-B.; Chavaria, D.; Plantier-Royon, R. *J. Org. Chem.* **2013**, *78*, 11477−11482. (c) Adams, D. J.; Clark, J. H.; Hansen, L. B.; Sanders, V. C.; Tavener, S. J. *J. Fluorine Chem.* **1998**, *92*, 123−125. (d) Yoshimatsu, M.; Kuribayashi, M. *J. Chem. Soc., Perkin Trans. 1* **2001**, 1256−1257. (e) Nozawa-Kumada, K.; Osawa, S.; Sasaki, M.; Chataigner, I.; Shigeno, M.; Kondo, Y. *J. Org. Chem.* **2017**, *82*, 9487−9496.

(74) Zefirov, N. S.; Makhon'kov, D. I. *Chem. Rev.* **1982**, *82*, 615−624.

(75) The kinetics for reactions of **2** (0.4 M) with **1b** (0.48 M) are again complicated by inhibitors. When initiated by 0.3 mM KOPh, the reaction is pseudo-zero-order throughout; this result is consistent with a number of mechanisms, including for example turnover and inhibition by **1b** or rate-limiting dissociation of CF$_3$ from dominant anion **B$_b$**. The faster rates of reaction with Bu$_4$N$^+$ versus K$^+$ as counterion suggest mechanism V*ii* dominates.